RESEARCH ARTICLE | FEBRUARY 02 2024

Machine learning based classification of vector field configurations

Special Collection: 68th Annual Conference on Magnetism and Magnetic Materials

Swapneel Amit Pathak ; Kurt Rahir ; Sam Holt ; Martin Lang ; Hans Fangohr

AIP Advances 14, 025004 (2024)
https://doi.org/10.1063/9.0000686

Machine learning based classification of vector field configurations

Cite as: AIP Advances 14, 025004 (2024); doi: 10.1063/9.0000686
Submitted: 1 October 2023 • Accepted: 22 November 2023 •
Published Online: 2 February 2024

Swapneel Amit Pathak,[1,2,a)] Kurt Rahir,[3] Sam Holt,[1,2] Martin Lang,[1,2,3] and Hans Fangohr[1,2,3]

AFFILIATIONS

[1] Max-Planck Institute for the Structure and Dynamics of Matter, Luruper Chaussee 149, 22761 Hamburg, Germany
[2] Center for Free-Electron Laser Science, Luruper Chaussee 149, 22761 Hamburg, Germany
[3] University of Southampton, Southampton SO17 1BJ, United Kingdom

Note: This paper was presented at the 68th Annual Conference on Magnetism and Magnetic Materials.
[a)] **Author to whom correspondence should be addressed:** swapneel-amit.pathak@mpsd.mpg.de

ABSTRACT

Magnetic materials at the nanoscale are important for science and technology. A key aspect for their research and advancement is the understanding of the emerging magnetization vector field configurations within samples and devices. A systematic parameter space exploration—varying for example material parameters, temperature, or sample geometry—leads to the creation of many thousands of field configurations that need to be sighted and classified. This task is usually carried out manually, for example by looking at a visual representation of the field configurations. We report that it is possible to automate this process using an unsupervised machine learning algorithm, greatly reducing the human effort. We use a combination of convolutional auto-encoder and density-based spatial clustering of applications with noise (DBSCAN) algorithm. To evaluate the method, we create the magnetic phase diagram of a FeGe disc as a function of changing external magnetic field using computer simulation to generate the configurations. We find that the classification algorithm is accurate, fast, requires little human intervention, and compares well against the published results in the literature on the same material geometry and range of external fields. Our study shows that machine learning can be a powerful tool in the research of magnetic materials by automating the classification of magnetization field configurations.

I. INTRODUCTION

Magnetic materials play important roles in domains ranging from geology to data storage and medicine. Computer simulation have enabled research advances in materials research in fundamental science and virtual design optimization in industry. A particular strength of the simulation based parameter space exploration is the ability to quickly generate many possible designs or magnetization configurations. The analysis and evaluation of such large datasets typically requires considerable human effort. In this work, we explore the suitability of Machine Learning (ML) to provide automatic classification of large sets of vector field configurations, in the context of vector fields describing magnetization fields.

ML is the branch of Artificial Intelligence which automates the process of approximating an analytical model from the provided data. ML has found numerous applications in physical sciences, for example in material discovery,[1] quantum chemistry,[2] protein folding,[3] molecular dynamics,[4] collider physics,[5] astrophysics,[6] plasma control in tokamak,[7] etc. In the field of magnetism, ML has been used in calculation of magnetization equilibrium states[8] and dynamics,[9] magnetic phase discovery,[10–13] etc. Particularly, the task of magnetic phase diagram construction[14,15] lends itself well to ML methods as the exploration of states is done with large amounts of data which needs to be clustered and classified.

Previous attempts at magnetic phase identification with ML have been focused on systems modeled using the Ising model.[10,11,13] A global phase exploration using the Ising Model was also undertaken by combining Principal Component Analysis (PCA) with an unsupervised clustering technique.[12]

Here, we repeat parts of a published study[14] to explore the suitability of ML-based classification of the simulation results to create the phase diagram computed in Ref. 14. Following the original

study, we use micromagnetic simulations to generate magnetization field configurations for a range of applied external fields in a disc geometry. The states are then clustered into different classes using an unsupervised clustering algorithm: density-based spatial clustering of applications with noise[16] (DBSCAN). First, a feature space of reduced dimensionality compared to the simulation results is obtained through a purpose-build convolutional auto-encoder. Next, we feed the feature space to the clustering algorithm to obtain different classes.

We find a good agreement of the clustering results we obtain using ML-assisted automatic classification when comparing with the published study in which the data was analyzed manually.

II. METHODS

Each vector field configuration $\mathbf{m}(\mathbf{r})$ under consideration is a mapping from a subregion $\mathbf{r} \in S \subset \mathbb{R}^3$ to a subregion $V \subset \mathbb{R}^3$ of space: $\mathbf{m} : \{S \to V, \mathbf{r} \mapsto \mathbf{m}(\mathbf{r})\}$. In our particular context of vector fields representing magnetization, the domain S is typically representing the magnetic material, or some discretized form of space containing magnetic material. The values of the vector field $\mathbf{m} \in V$ are generally limited in magnitude by the saturation magnetization. For the micromagnetics used here $\mathbf{m}$ is normalized so that $|\mathbf{m}| = 1$ (Sec. II A).

The simulations were performed using the `ubermag`[17] Python meta-package for finite-difference micromagnetic simulations, which uses `OOMMF`[18] for energy minimization. For training the auto-encoder we use `tensorflow`[19,20] and for clustering we use `scikit-learn`.[21]

A. Micromagnetic simulations

We consider a FeGe disc geometry of diameter 160 nm and thickness 10 nm. The different equilibrium states are obtained in the presence of an external magnetic field ($\mu_0\mathbf{H}$) along the positive z axis. Simulations are performed for 345 randomly chosen field strengths between 0 T and 1.2 T. We take into account energy contributions from the ferromagnetic exchange interaction, Dzyaloshinskii–Moriya interaction (DMI), external magnetic field and demagnetization field:

$$E = \int_V \left[-A\mathbf{m} \cdot \nabla^2 \mathbf{m} + D\mathbf{m} \cdot (\nabla \times \mathbf{m}) - \mu_0 M_s \mathbf{m} \cdot \mathbf{H} - \frac{1}{2}\mu_0 M_s \mathbf{m} \cdot \mathbf{H}_d \right] \mathrm{d}V.$$

Here, $\mathbf{m}$ is the normalized magnetization vector field, A is the exchange stiffness constant, D is the DMI constant, M_s is the saturation magnetization, $\mathbf{H}$ is the external magnetic field, and $\mathbf{H}_d$ is the demagnetization field of the material.

The total energy of the system is minimized using a conjugate gradient algorithm to obtain an equilibrium magnetization configuration. It is important to note that the equilibrium state thus obtained depends strongly on the initial (starting) configuration. Hence, in order to obtain a full set of configurations possible in the system, the simulations at each external field value are initiated

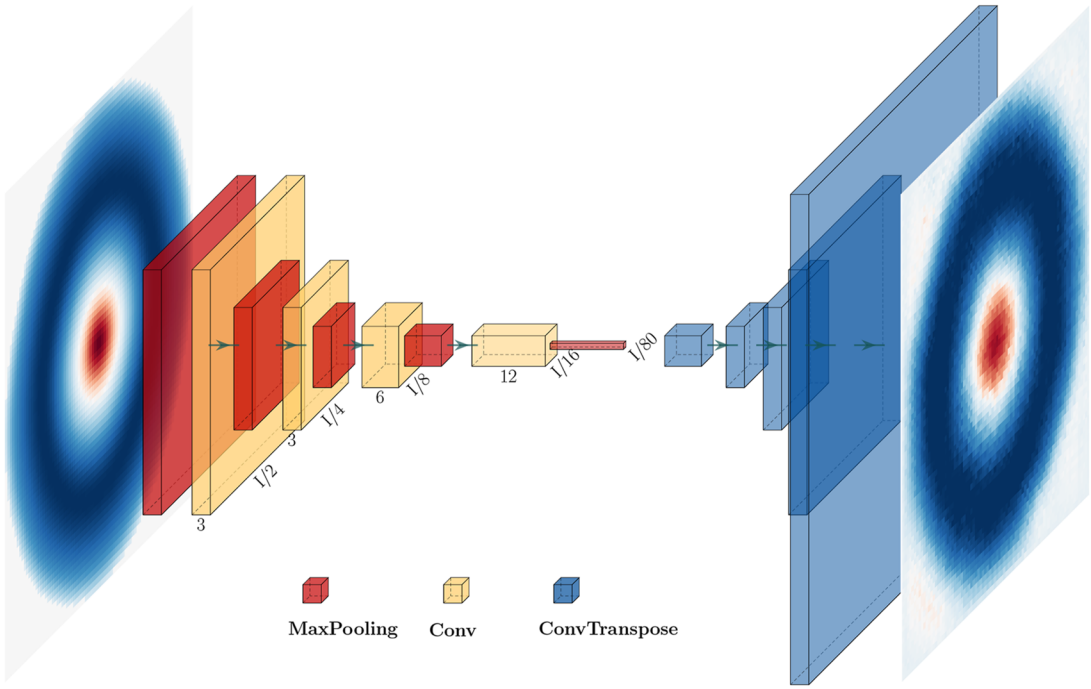

FIG. 1. Convolutional auto-encoder architecture used to reduce the dimensionality of the simulation magnetization array from 19200 (80 × 80 × 3) to 12 (12 × 1). The input array is a simulated magnetization configuration, for example a skyrmion state. The auto-encoder is expected to reduce the dimensions of the feature space (encoder), and subsequently recreate the input from the space of reduced dimensionality (decoder) as the output. Hence, in the training process it learns a meaningful representation of the data in a lower dimensional space. The exact architecture of the auto-encoder is provided in the supplementary material.[22]

from several different magnetization configurations representing the analytical solutions of the magnetization configurations of the given energy contributions.[14,22]

To discretize the geometry, we create a mesh of cubic cells of size 2 nm, which is well below the exchange length (≈10nm) and long-range helical period (≈70nm) of the material. The magnetization vector fields **m** of the equilibrium states for changing external field values are stored as `omf` files and the corresponding value of external field and total energy in `json` files.

The material parameters[14] used to simulate FeGe are $A = 8.78 \times 10^{-12}$ J m^{-1}, $D = 1.58 \times 10^{-3}$ J m^{-2}, and $M_s = 384$ kAm^{-1}. We have 3010 equilibrium states in total, which are to be clustered into individual classes based on their magnetization configuration.

B. Dimensionality reduction: Auto-encoder

With the simulation cell size of 2 nm for a disc of diameter 160 nm and thickness 10 nm, the simulation result **m** is given by a $80 \times 80 \times 5 \times 3$ array representing the magnetization field on $80 \times 80 \times 5$ spatial discretization points, each providing three components for the local **m** vector. We consider only a slice of the **m**-field at the center of the disc thickness for the clustering task. Since the thickness of the disc is small compared to the length scales at which one expects to observe inhomogeneities in the magnetization for this material, a central slice is a reasonable representation of the full configuration. This reduces the dimensionality of the feature space by a factor of five to $80 \times 80 \times 3$, however, the resulting space is still 19200 dimensional. Clustering on data with dimensionality this high can lead to poor results: often referred to as the *curse of dimensionality*. To elaborate, the high dimensional data is at the risk of being very sparse in the feature space if the number of instances are not high enough. This can negatively impact the performance of a clustering algorithm. Moreover, the computation time of the clustering can improve significantly if the dimensionality of the feature space is reduced. In the micromagnetic framework, the magnetization field is changing slowly in space. Hence, magnetization vectors in nearby cells are highly correlated, which indicates the theoretical possibility of dimensionality reduction.

For the dimensionality reduction, we employ a convolutional auto-encoder.[23] We feed the simulation results as the input and expect the same as the output (Fig. 1). The architecture and the number of trainable parameters of the first half (encoder) and the second half (decoder) of the auto-encoder are kept as close to each other as possible.[22] We use mean squared error (MSE) as the loss function

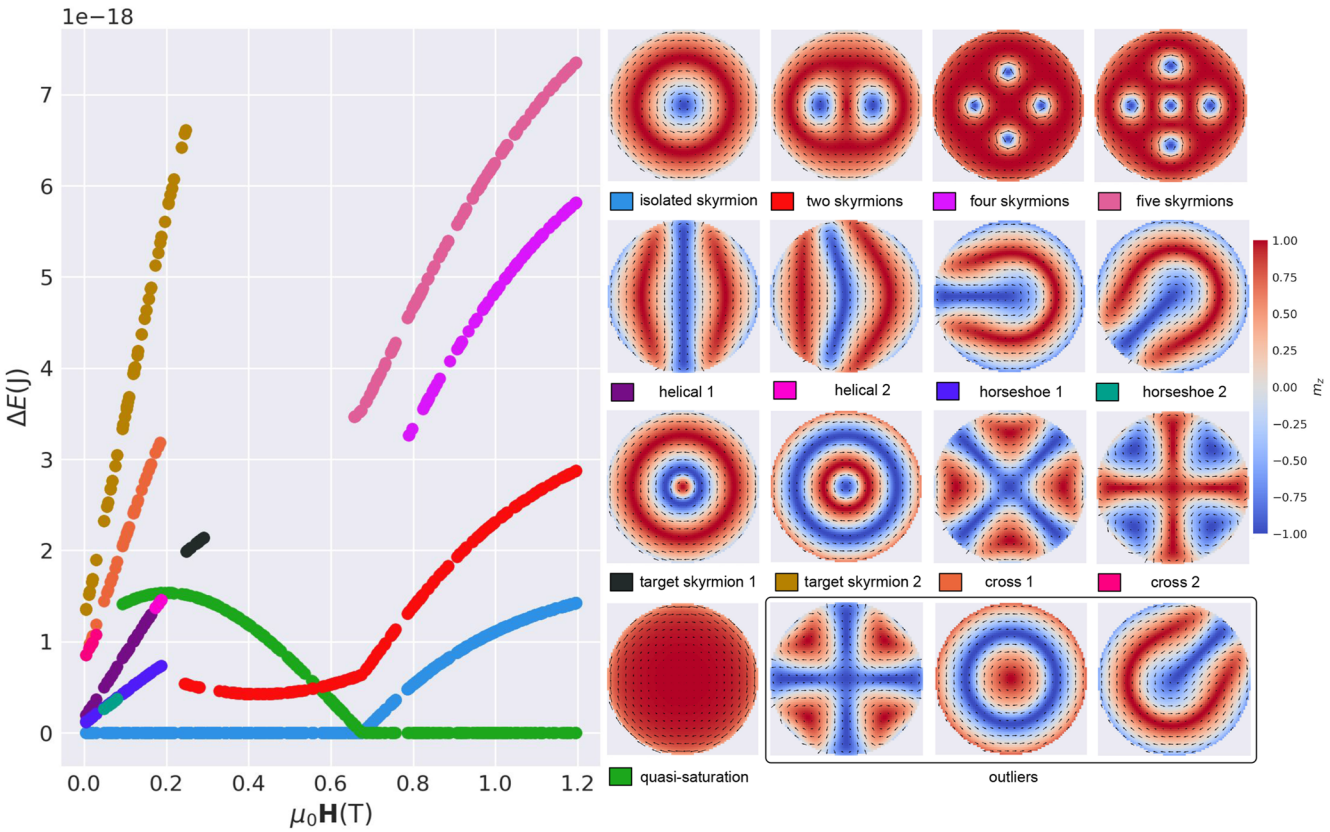

FIG. 2. Magnetization configurations of 13 different clustered classes and their distribution as a function of changing external field (μ_0**H**). The *y* axis shows the energy difference of a given configuration with respect to the ground state at that external field. Additionally to the clustered classes, we obtain outlier configurations, which are not part of any class. We find the results to be in a good agreement with the Fig. 3b of Ref. 14 of the published study on the same material geometry and range of external fields.

and the adaptive moment estimation (ADAM)[24] optimizer for training the network. For the optimizer, the learning rate is initialized to 0.001, the momentum decay hyper-parameter β_1 to 0.9, and the scaling decay hyper-parameter β_2 to 0.999.

Once the auto-encoder is trained to a sufficient accuracy, the encoder is used to obtain the feature space of reduced dimensionality. We find that it is possible to reduce the dimensionality from 19200 to 12 (Fig. 1) without impacting the MSE of the auto-encoder.

C. Clustering: DBSCAN

We use DBSCAN to cluster the feature space. The algorithm clusters on the basis of density of instances in a neighborhood in the feature space. It calculates the number of instances within an ε Euclidean distance of an instance. If the number of instances are greater than a specified minimum number of instances, the instance becomes a core instance of a class and the instances in the neighborhood become the members of that class. Hence, the two hyper-parameters ε and the minimum number of instances needs to be optimized for the clustering task.

Since the number of configurations in our case are relatively small, one can use a small number for the minimum instances to create individual classes. We find that a value of 5 for the minimum instances works well in our case. An intuition for the value of the ε distance is obtained by plotting the distribution of the distances of the 5th nearest-neighbors of each instance in the feature space in an ascending order.[16] For our case, a value of 0.86 works well for ε. However, it is important to note that this value will change depending on the different models used for the dimensionality reduction. Hence, it is always advisable to plot the distribution of distances to get an intuition of this value.

Using these hyper-parameters for the DBSCAN clustering, we obtain 13 classes (Fig. 2) which are discussed below.

III. RESULTS

The magnetization configurations and the distribution of the clustered classes as a function of external magnetic field are shown in Fig. 2. The left plot shows the energy differences of the individual equilibrium states with respect to the ground state at a given external field. Using this approach, it is possible to clearly identify the different classes visually as they form distinct trend lines. This is useful in determining the accuracy of the clustering algorithm visually. Moreover, the plot helps in making a one-to-one comparison with the published study.

As mentioned earlier, we obtain 13 different clusters of equilibrium configurations: isolated skyrmion, two skyrmions, four skyrmions, five skyrmions, target skyrmion 1 and 2, helical type 1 and 2, horseshoe type 1 and 2, *cross* type 1 and 2, and quasi-saturation state. The algorithm also produced six outlier configurations, which are not part of any of the clusters, with three unique configurations as shown in Fig. 2. Within each of the 13 clustered classes, we find no intermixing of magnetization configurations, i.e., all the instances of a given class are visually similar.

The configurations found in the automatic classification agree well with the published study[14] on the same material geometry. The trend lines corresponding to the isolated skyrmion, two skyrmions, target skyrmion 2, helical type 1, and quasi-saturation state are in very good agreement with Fig. 3b of Ref. 14. The study here identifies and reports additional configurations, such as the 4 and 5 skyrmion configurations which were outside the scope of the Ref. 14. Our study did not find 3-skyrmion configurations. This might be due to our study using finite difference simulations whereas finite element discretization was used in Ref. 14. We note that there is a slight difference in the initial configurations used to obtain the equilibrium configurations in both the studies.

We note the absence of rotational invariance in the clustered classes (e.g., the two horseshoe type states are identified as separate classes). A possible reason for this can be the auto-encoder being insensitive to the rotational symmetry of the system since the no effort has been made to address this during the training process.

The study was performed on Intel(R) Xeon(R) CPU E5-2670 @ 2.60 GHz with 16 physical cores and 24GB of RAM. The wall time for training the auto-encoder was 35 s and for clustering the feature space using DBSCAN was 8.04 **µ**s.

IV. CONCLUSION AND OUTLOOK

The study shows that machine learning can be a powerful tool to automate the process of vector field classification. We demonstrate this here for the classification of equilibrium magnetization states in the study of magnetic materials. We find that the method is accurate, fast, and requires no human supervision (other than tuning hyperparameters). ML-assisted classification can substantially ease the time-consuming and error-prone task of manual analysis of large simulation datasets.

Due to the flat geometry for the disc studied here, we have assumed that the magnetization does not vary substantially along the z-direction, and thus treated the system as essentially two dimensional in the x-y plane (although the vectors defined at those positions have three components). Going forward, a natural next step is to investigate clustering of magnetization configurations that are defined in 3 dimensions.

Another avenue of further exploitation is to use the approach to classify experimentally obtained datasets.

ACKNOWLEDGMENTS

This work was financially supported by the EPSRC UK Skyrmion Project Grant EP/N032128/1. We are grateful for useful discussions with Andreas Marek and team members from the Max Planck Compute and Data Facility.

AUTHOR DECLARATIONS

Conflict of Interest

The authors no conflicts to disclose.

Author Contributions

Swapneel Amit Pathak: Conceptualization (lead); Investigation (lead); Methodology (lead); Software (equal); Visualization (equal); Writing – original draft (lead); Writing – review & editing (equal). **Kurt Rahir**: Conceptualization (equal); Investigation (equal);

Methodology (equal); Software (equal); Visualization (equal). **Sam Holt**: Conceptualization (equal); Investigation (equal); Methodology (equal); Software (equal); Visualization (equal); Writing – review & editing (equal). **Martin Lang**: Methodology (supporting); Software (equal); Visualization (equal); Writing – review & editing (equal). **Hans Fangohr**: Conceptualization (equal); Funding acquisition (lead); Investigation (supporting); Methodology (supporting); Project administration (lead); Resources (lead); Software (supporting); Supervision (lead); Writing – review & editing (equal).

DATA AVAILABILITY

All the relevant data and software is available online.[22]

REFERENCES

[1] Y. Liu, T. Zhao, W. Ju, and S. Shi, "Materials discovery and design using machine learning," Journal of Materiomics **3**, 159–177 (2017).

[2] J. Kirkpatrick, B. McMorrow, D. H. Turban, A. L. Gaunt, J. S. Spencer, A. G. Matthews, A. Obika, L. Thiry, M. Fortunato, D. Pfau *et al.*, "Pushing the frontiers of density functionals by solving the fractional electron problem," Science **374**, 1385–1389 (2021).

[3] J. Jumper, R. Evans, A. Pritzel, T. Green, M. Figurnov, O. Ronneberger, K. Tunyasuvunakool, R. Bates, A. Žídek, A. Potapenko *et al.*, "Highly accurate protein structure prediction with alphafold," Nature **596**, 583–589 (2021).

[4] Y. Wang, J. M. L. Ribeiro, and P. Tiwary, "Machine learning approaches for analyzing and enhancing molecular dynamics simulations," Current opinion in structural biology **61**, 139–145 (2020).

[5] A. J. Larkoski, I. Moult, and B. Nachman, "Jet substructure at the large hadron collider: A review of recent advances in theory and machine learning," Physics Reports **841**, 1–63 (2020).

[6] Ž. Ivezić, A. J. Connolly, J. T. VanderPlas, and A. Gray, "Statistics, data mining, and machine learning in astronomy," in *Statistics, Data Mining, and Machine Learning in Astronomy* (Princeton University Press, 2014).

[7] J. Degrave, F. Felici, J. Buchli, M. Neunert, B. Tracey, F. Carpanese, T. Ewalds, R. Hafner, A. Abdolmaleki, D. de Las Casas *et al.*, "Magnetic control of tokamak plasmas through deep reinforcement learning," Nature **602**, 414–419 (2022).

[8] B. Trenchev, S. Dasmahapatra, M. Beg, O. Hovorka, and N. Downing, "Generating magnetic skyrmion ground states with generative adversarial networks," in *Third Workshop on Machine Learning and the Physical Sciences* (NeurIPS, 2020).

[9] A. Kovacs, J. Fischbacher, H. Oezelt, M. Gusenbauer, L. Exl, F. Bruckner, D. Suess, and T. Schrefl, "Learning magnetization dynamics," Journal of Magnetism and Magnetic Materials **491**, 165548 (2019).

[10] S. Acevedo, M. Arlego, and C. A. Lamas, "Phase diagram study of a two-dimensional frustrated antiferromagnet via unsupervised machine learning," Physical Review B **103**, 134422 (2021),

[11] B. Çivitcioğlu, R. A. Römer, and A. Honecker, "Machine learning the square-lattice Ising model," Journal of Physics: Conference Series **2207**, 012058 (2022).

[12] D. R. de Assis Elias, E. Granato, and M. de Koning, "Global exploration of phase behavior in frustrated Ising models using unsupervised learning techniques," Physica A: Statistical Mechanics and its Applications **589**, 126653 (2022).

[13] J. Carrasquilla and R. G. Melko, "Machine learning phases of matter," Nature Physics **13**, 431–434 (2017).

[14] M. Beg, R. Carey, W. Wang, D. Cortés-Ortu ño, M. Vousden, M.-A. Bisotti, M. Albert, D. Chernyshenko, O. Hovorka, R. L. Stamps *et al.*, "Ground state search, hysteretic behaviour and reversal mechanism of skyrmionic textures in confined helimagnetic nanostructures," Scientific reports **5**, 17137 (2015).

[15] S. A. Pathak and R. Hertel, "Three-dimensional chiral magnetization structures in FeGe nanospheres," Physical Review B **103**, 104414 (2021).

[16] M. Ester, H.-P. Kriegel, J. Sander, X. Xu *et al.*, "A density-based algorithm for discovering clusters in large spatial databases with noise," in *KDD* (AAAI Press, 1996), Vol. 96, pp. 226–231.

[17] M. Beg, M. Lang, and H. Fangohr, "Ubermag: Towards more effective micromagnetic workflows," IEEE Transactions on Magnetics **58**, 7300205 (2022).

[18] M. J. Donahue and M. Donahue, OOMMF User's Guide, Version 1.0, 1999.

[19] M. Abadi, A. Agarwal, P. Barham, E. Brevdo, Z. Chen, C. Citro, G. S. Corrado, A. Davis, J. Dean, M. Devin, S. Ghemawat, I. Goodfellow, A. Harp, G. Irving, M. Isard, Y. Jia, R. Jozefowicz, L. Kaiser, M. Kudlur, J. Levenberg, D. Mané, R. Monga, S. Moore, D. Murray, C. Olah, M. Schuster, J. Shlens, B. Steiner, I. Sutskever, K. Talwar, P. Tucker, V. Vanhoucke, V. Vasudevan, F. Viégas, O. Vinyals, P. Warden, M. Wattenberg, M. Wicke, Y. Yu, and X. Zheng, "TensorFlow: Large-scale machine learning on heterogeneous systems," 2015, software available from tensorflow.org.

[20] F. Chollet *et al.*, "Keras," https://keras.io, 2015.

[21] F. Pedregosa, G. Varoquaux, A. Gramfort, V. Michel, B. Thirion, O. Grisel, M. Blondel, P. Prettenhofer, R. Weiss, V. Dubourg, J. Vanderplas, A. Passos, D. Cournapeau, M. Brucher, M. Perrot, and E. Duchesnay, "Scikit-learn: Machine learning in Python," Journal of Machine Learning Research **12**, 2825–2830 (2011).

[22] S. A. Pathak, S. Holt, M. Lang, and H. Fangohr, "Supplementary material: Machine learning based classification of vector field configurations," 2023, https://gitlab.mpcdf.mpg.de/fangohr/paper-2023-machine-learning-based-classification-of-magnetization.

[23] J. Masci, U. Meier, D. Cireşan, and J. Schmidhuber, "Stacked convolutional auto-encoders for hierarchical feature extraction," in *Artificial Neural Networks and Machine Learning–ICANN 2011: 21st International Conference on Artificial Neural Networks, Espoo, Finland, June 14-17, 2011, Proceedings, Part I 21* (Springer, 2011), pp. 52–59.

[24] D. P. Kingma and J. Ba, "Adam: A method for stochastic optimization," arXiv:1412.6980 (2014).